Separation and Purification Technology 316 (2023) 123814

Contents lists available at ScienceDirect

Separation and Purification Technology

journal homepage: www.elsevier.com/locate/seppur

# Fouling of ion-exchange membranes during electrodialytic acid whey processing analysed by 2D fluorescence and FTIR spectroscopy

Emilie N. Nielsen [a], Ulysse Cordin [b], Mathias Gøtke [a], Svetlozar Velizarov [c], Claudia F. Galinha [c], Leif H. Skibsted [a], João G. Crespo [c], Lilia M. Ahrné [a,*]

[a] Department of Food Science, University of Copenhagen, Rolighedsvej 26, 1958 Frederiksberg, Denmark
[b] Agrocampus OUEST, 65 rue de Saint Brieuc – CS 84215, 35042 Rennes Cedex, France
[c] LAQV REQUIMTE, Department of Chemistry, NOVA School of Science and Technology, FCT NOVA, Universidade NOVA de Lisboa, 2829-516 Caparica, Portugal

ARTICLE INFO

*Keywords:*
Electrodialysis
Fouling
Ion-exchange membranes
Acid whey
2D fluorescence spectroscopy
FTIR

ABSTRACT

Acid whey (AW), a by-product from the production of acidified dairy products, contains high amounts of lactic acid and minerals that can be recovered by electrodialysis (ED). To better understand the process and improve its efficiency, the objective of this study was to investigate fouling of ion-exchange membranes (IEMs) during ED of AW and concentrated AW by reverse osmosis (ROAW), underlimiting (ULCD), limiting (LCD) and overlimiting current density operating conditions (OLCD). The structure, hydrophobicity, and chemical composition of membranes showed differences regarding fouling on anion- (AEM) and cation- (CEM) exchange membranes facing the diluate and the concentrate, both for AW and ROAW. Furthermore, operating at OLCD tends to reduce fouling compared to ULCD, due to the expected generation of electroconvective vortices. 2D fluorescence spectroscopy and Fourier-transform infrared spectroscopy (FTIR) provided complementary and more detailed information regarding the fouling and efficiency of the cleaning procedure. The 2D fluorescence spectra showed that the AEM surfaces in contact with the diluate change more than those in contact with the concentrate. The FTIR analyses showed the presence of lactose and lactic acid on the AEM surfaces in contact with the concentrate, which could not be detected by fluorescence.

## 1. Introduction

To improve the sustainable food industry, in the last years, special attention has been given to valorization of side streams [1]. A major side stream from the dairy industry is acid whey (AW), which is a by-product from the production of e.g. skyr, quark, Greek yoghurt and cottage cheese. It contains high concentration of minerals, lactic acid and lactose but low concentration of proteins [2]. The presence of high concentration of lactic acid and minerals hinders the crystallization of lactose, and conversion of AW into a stable powder with a long shelf life [3,4]. Several studies have shown that electrodialysis (ED) is an efficient technology to separate charged compounds from AW [2,5–7], increasing the stability of the resulting powder [8]. However, as common in membrane separation processes, a large limitation of ED is fouling of the ion-exchange membranes (IEMs) [6,7], that limits the process separation efficiency. Especially calcium and magnesium, which are found in high concentrations in AW, are known for causing severe fouling on IEMs [9,10]. Several strategies have been investigated to minimize fouling during ED. Dufton and co-authors [7] compared direct current with pulsed electric field, and found that the use of the latter decreases both the fouling of the membranes and energy consumption. However, selecting the right pulse/pause combination is of crucial importance to obtain good results. The same group has also compared two electrodialysis configurations, one conventional and one using bipolar membranes, regarding IEMs fouling during AW deacidification and concluded that the degree and type of fouling depends on the configuration [6]. Furthermore, the applied current density affected the degree of organic fouling. Persico and co-authors [11] found that operating at overlimiting current density (OLCD) conditions decreases peptide fouling on IEMs. It was suggested that the generation of $H^+$ and $OH^-$ ions during water splitting, taking place during operation at OLCD conditions, causes both the neutralization of peptides charges and generation of electroconvective vortices at the membranes interface, which reduce attachment of peptides to the membranes. However, the water splitting

* Corresponding author.
*E-mail addresses:* Emilie.nyborg@food.ku.dk (E.N. Nielsen), ulysse1054@gmail.com (U. Cordin), mathiasgoetke@gmail.com (M. Gøtke), s.velizarov@fct.unl.pt (S. Velizarov), cf.galinha@fct.unl.pt (C.F. Galinha), jgc@fct.unl.pt (L.H. Skibsted), ls@food.ku.dk (J.G. Crespo), Lilia@food.ku.dk (L.M. Ahrné).

https://doi.org/10.1016/j.seppur.2023.123814
Received 3 January 2023; Received in revised form 5 March 2023; Accepted 6 April 2023
Available online 8 April 2023

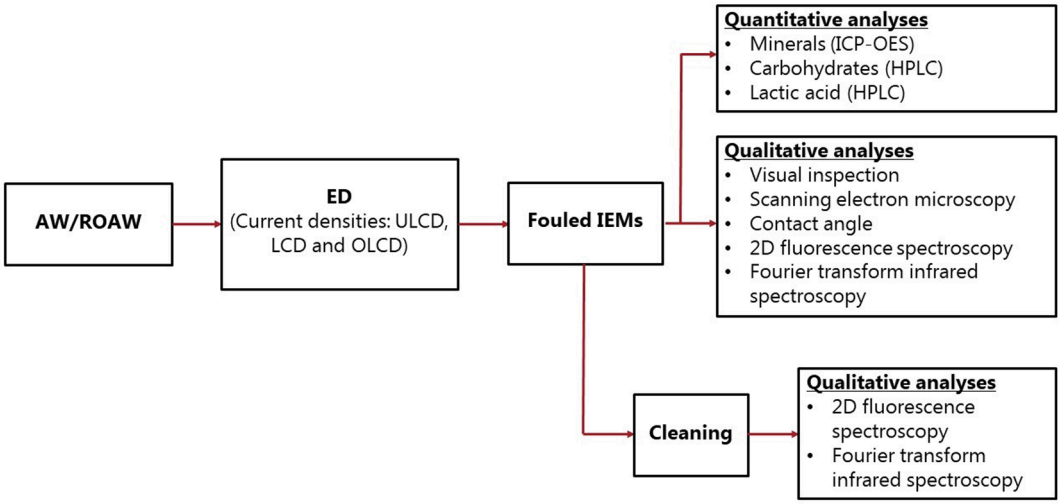


**Fig. 1.** Overview of the experimental design of the study. AW, acid whey; ROAW, RO pre-processed acid whey retentate; ED, electrodialysis; ULCD, underlimiting current density; LCD, limiting current density; OLCD, overlimiting current density; IEM, ion-exchange membrane.

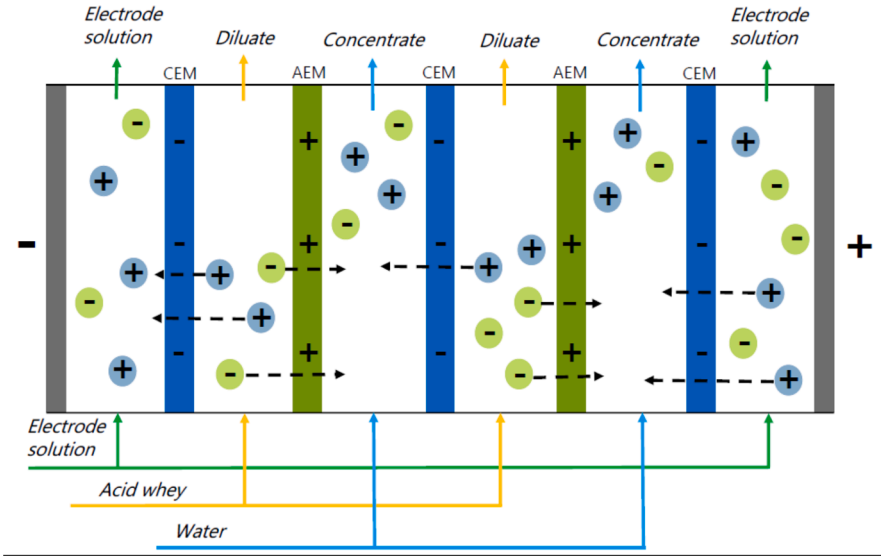


**Fig. 2.** Schematic representation of ED operation principle.

results in the generation of $H^+$ and $OH^-$ ions, which strongly affects the pH in the diluate and concentrate streams and thereby the solubility of the present minerals [12].

A previous study of Pawlowski and co-authors [13] has shown that two-dimensional (2D) fluorescence spectroscopy has a high potential for studying fouling development on IEMs during reverse ED. Fluorescence spectroscopy is a non-invasive technique which can be used to detect fluorophores such as amino acids, vitamins and aromatic organic matter [14], and has been used to detect chemical and physical changes in dairy products [15]. When the fluorophores are excited they emit light, which can be detected by fluorescence spectroscopy. Recent studies have also shown that Fourier transform infrared spectroscopy (FTIR) can be used to detect fouling and changes in IEMs [16,17]. Fourier-transform infrared spectroscopy (FTIR) is a vibrational spectroscopic technique which can detect functional groups, types of bonding and give information about molecular conformations [18]. A change in dipole moment of the bond in the analysed molecule as a result of the vibration that occurs when IR radiation is absorbed, excites the electrons in the bonds to a higher vibration state, causing bending or stretching motions of the molecular bonds [19]. FTIR has successfully been used to detect food compounds, such as sugars and lactic acid [20,21], which are present in high concentrations in AW [2].

AW is a complex side stream, with high concentrations of both organic and inorganic matter. Typically, reverse osmosis (RO) is used to concentrate dairy products, such as AW to reduce the water content and thereby the volume during transport from dairies producing the AW to dairies producing ingredients. Therefore, it is of high interest to investigate how operating the ED at different current density conditions affects the process performance of the IEMs. 2D fluorescence and FTIR spectra are quick to obtain and nondestructive to the membrane. By combining the scans at membrane surface using the PCA algorithm we hypothesized that is possible to understand and compare the effect of operating conditions and cleaning methods on the membrane surfaces. Other inspection techniques are more time- and labor-consuming, involve the use of chemical reagents, require a pre-knowledge about potential foulants and are not able to provide a complete overview of the membrane surface and positioning the status of the membrane within other membrane samples. Thus, the objective of the present study was to investigate fouling of IEMs during ED processing of AW and reverse osmosis (RO) concentrated AW (ROAW) by analyzing the structure,

**Table 1**
Standard cleaning procedure of ion-exchange membranes.

| Step of cleaning | Cleaning solution | Time (min) |
|---|---|---|
| 1 | Deionized water | 30 |
| 2 | 1% HCl | 30 |
| 3 | Deionized water | 30 |
| 4 | 1% NaOH | 30 |
| 5 | Deionized water | 30 |

hydrophobicity, and chemical composition of fouling in combination with spectrometric methods, such as 2D fluorescence spectroscopy and FTIR. The ED process was performed at underlimiting current density (ULCD), limiting current density (LCD) and overlimiting (OLCD) to assess the effect of current density on the fouling formation. Additionally, the efficiency of the cleaning procedure of the fouled IEMs was evaluated using 2D fluorescence spectroscopy and FTIR.

## 2. Materials and methods

### 2.1. Experimental overview

An overview of the experimental design is shown in Fig. 1. The ED was performed in duplicates.

### 2.2. Acid whey

AW from the production of conventional skyr was obtained from Arla Foods (Hobro, Denmark). The composition of the AW was: lactose 34.33 ± 1.76 ($gL^{-1}$), lactic acid 9.39 ± 0.39 ($gL^{-1}$), protein 0.17 ± 0.01 % wb, total solids 5.92 ± 0.28% wb, ashes 0.64 ± 0.01% wb, further details about specific minerals can be found in Nielsen and co-authors [2]. After receiving, the AW was immediately concentrated by RO or stored in a freezer at −20 °C until further use.

### 2.3. Concentration of acid whey by reverse osmosis

AW (90 L) was concentrated by TFC™ HRX™ 2538 HRX-VYV RO membranes, in a spiral wound module (with an effective area of 1.8 $m^2$) from Koch Membrane Systems (Stafford, UK) using a MMS SW25 pilot filtration plant from MMS AG Membrane Systems (Urdorf, Switzerland). The concentration temperature was 50 °C and the TMP was 30 bar. The AW was concentrated until a mass concentration factor of 2.5 was reached. The AW RO concentrate was stored until further use at −20 °C.

### 2.4. Electrodialysis configuration

An EDR-Z/10–0.8 ED unit (MemBrain s.r.o., Stráž pod Ralskem, Czech Republic) was used for the ED experiments. The unit was equipped with 10 pairs of heterogeneous AM-PES (AEM, anionic) and CM-PES (CEM, cationic) ion-exchange membranes Ralex® (MEGA a.s., Stráž pod Ralskem, Czech Republic) in CEM-AEM-CEM configuration (Fig. 2) with a total membrane area of 13.44 × $10^{-2}$ $m^2$. The first CEM and AEM were removed after each test, and replaced by new IEMs, before they were dried and analysed for fouling. The properties of the membranes can be found in Merkel and Ashrafi [22]. The electrical potential was applied to Pt coated titanium electrodes. The voltage on the membrane stack was measured between two Pt wires, which were connected to the end of the stack. The temperature of the ED process was controlled by an ice water bath.

### 2.5. Limiting current density

The LCD of the ED systems when demineralizing AW and ROAW were determined using the Cowan and Brown method [23]. Two kg AW or ROAW, 0.75 kg tap water and 0.25 kg ≥ 99 % $Na_2SO_4$ (20 g/L) (Merck KGaA, Darmstadt, Germany) were used in the ED stack, respectively as diluate, concentrate and electrodes' rinse solutions. The concentrate pH was adjusted to 6.5 with 1 % (v/v) HCl (analytical grade) to prevent mineral precipitation. All solutions were circulated at a constant flow rate of 55 L/h each. The voltage was increased by increments of 1 V from 0 to 35 V and held by 2 min. After each increment the voltage was turned off for 3 min. The values of voltage and current were plotted as resistance (U/I) as a function of reciprocal current (1/I). The limiting intensity values were found to be 0.62 ± 0.01 A and 0.83 ± 0.02 A for AW and ROAW, which corresponds to LCD of 9.7 ± 0.2 mA/$cm^2$ and 12.8 ± 0.3 mA/$cm^2$. All tests were made in duplicates.

### 2.6. Electrodialysis protocol and sampling of the membranes

The ED experiments were performed using 2 kg of diluate which consisted of either AW or ROAW, 0.75 kg tap water used as concentrate and 0.25 kg ≥ 99% $Na_2SO_4$ (20 g/L) (Merck KGaA, Darmstadt, Germany) for the electrode rinse solution. The diluate, concentrate and electrode rinse solution were circulated in the ED stack at a constant flow of 55 L/h each. The temperature was maintained at 20 °C using a water bath, and the pH of the concentrate solution was adjusted with 1% (v/v) HCl (analytical grade) to maintain the initial pH at 6.5 in order to prevent precipitation of calcium complexes, which are the most abundant minerals. The ED unit was operated using constant current manually adjusting the voltage. The current densities of the experiments were determined from the LCD test. The experiments started at ULCD was set to 50% below the found LCD, while the current density of the experiments started at OLCD was set to 40% above the LCD. During the experiments the pH, conductivity and temperature of the diluate and concentrate solutions were monitored in-line by HQ40d multimeters from Hach (Copenhagen, Denmark). The experiments ended when a 95% demineralization based on conductivity was reached, in order to follow as long as possible the ED process operation under specific process conditions. The ED process duration ranged from 90 min up to 275 min depending on the conditions used. The pH in the diluate changed from 4.45 to 3.75 while in the concentrate it changed from 6.5 to 4.5. After the ED experiments and before the cleaning in place (CIP), the two first membranes (AEM and a CEM) facing the anode were collected from the ED stack, photographed from each of their two sides and hanged to air dried at room temperature 25 °C: relative humidity of 50% for overnight before analysis. In the next day, the membranes (16 × 4 cm) were carefully cut in 5 strips (3 × 4 cm) using a paper cut to avoid loss of fouled material. The middle strip was used for mineral analysis, the second from the top for lactic acid and lactose analysis and the second from the bottom for water contact angle measurements and microscopy. The top and bottom strips were both used for 2D fluorescence spectroscopy and Fourier transform infrared spectroscopy. Pristine AEM and CEM were used as references for the IEMs. The experiments were performed in duplicates.

### 2.7. Cleaning procedure

The cleaning procedure of IEMs was performed following the recommendations from the IEMs supplier (MemBrain s.r.o., Stráž pod Ralskem, Czech Republic), as described in Table 1. The cleaning solution was circulated under high agitation at room temperature. The HCl and NaOH were of analytical grade.

### 2.8. Scanning electron microscopy

The membranes were coated with a thin layer of gold using an EM ACE200 Coating system (Leica Microsystems CMS GmbH) before the images were taken using a Quanta 200 Scanning Electron Microscope (SEM) from FEI Company with a magnification of 500x, accelerating voltage of 10.0 kV and a working distance of ~25 mm.

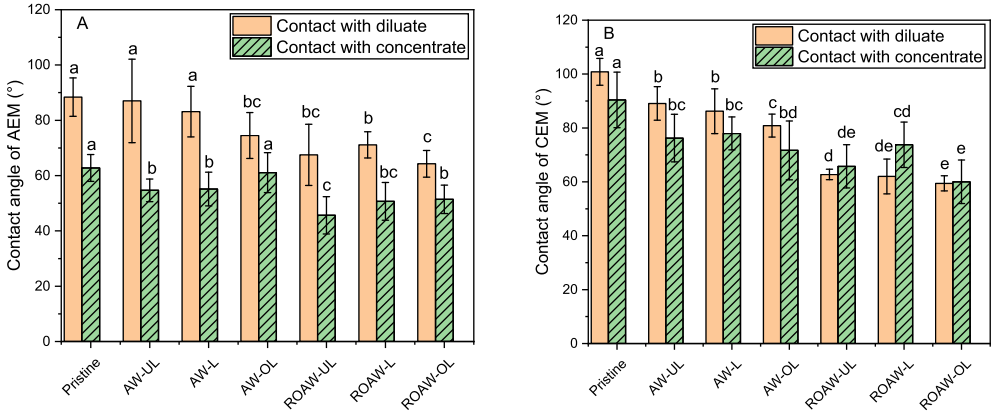


**Fig. 3.** Contact angle of A) AEM and B) CEM using underlimiting current density (UL), limiting current density (L) and overlimiting current density (OL) to treat acid whey (AW) and RO pre-processed acid whey (ROAW). The pristine membranes were tested after CIP. Means with different letters in the same column are significantly different ($p < 0.05$).

### *2.9. 2D fluorescence spectroscopy*

The result of 2D fluorescence spectroscopy measurements is excitation-emission matrices (EEMs), where the fluorescence emission intensity corresponding to excitation/emission wavelengths were recorded [41,42,43]. The EEMs were obtained of the dry IEMs with a fluorescence spectrophotometer Varian Cary Eclipse equipped with excitation and emission monochromators and coupled to an optical fiber bundle probe as described in Pawlowski and co-authors [13]. The scanning speed was 12 000 nm/min; excitation and emission slits were 10 and 5 nm, respectively. EEMs were generated in a range of 250–590 nm of excitation and 260–600 nm of emission, with an excitation incrementing step of 5 nm. Each IEM was measured with 2D fluorescence spectroscopy at least 3 times on each side. The distance between the IEM samples and the optical probe was maintained constant ( ~ 1 cm) in all measurements. The angle between the IEM surface and the optical probe was 45° to avoid an overlap of the excitation and emission light signals. All measurements were done in triplicates for each membrane, and each experiment in duplicate, resulting in at least 6 measurements for each membrane/condition.

### *2.10. Fourier transform infrared spectroscopy*

The Fourier transform infrared spectroscopy (FTIR) spectra of the membranes obtained, following a method adapted from Cifuentes-Cabezas and co-authors [43], using a FTIR Spectrometer from PerkinElmer (Waltham, MA, USA) equipped with an attenuated total reflection cell in absorption mode from 400 to 4000 $cm^{-1}$ with 4 accumulations scans and a resolution of 10 $cm^{-1}$ All measurements were done in triplicates for each membrane, and each experiment in duplicate, resulting in at least 6 measurements for each membrane/condition.

### *2.11. Water contact angle*

The contact angles of the fouled membranes and a new cleaned membrane were measured using a goniometer OCA 25 (DataPhysics Instruments GmbH, Filderstadt, Germany) to determine the hydrophobicity of the membrane surfaces, according to the method described by Persico and co-authors [11]. The membranes were hanged to air dry overnight before analysis, in order to remove surface water. A membrane was fixed in a flat position on the holding platform, and a droplet of MiliQ water was dispersed at its surface. An image of the droplet on the surface of the membrane was taken and used to determine the contact angle value. The contact angle was measured seven times for each membrane at different spots, and the measurement were made at room temperature.

### *2.12. Mineral composition on membranes*

The mineral composition on the membranes was adapted from Dufton and co-authors (2018) [6]. A piece of membrane with an area of 23.1 $cm^2$ was heated at 550 °C in a furnace (Nabertherm GmbH, Bremen, Germany) for 24 h. The burnt membrane was dissolved in 25% $HNO_3$ (Th. Geyer GmbH & Co. KG, Renningen, Germany) and diluted with MiliQ water to an acid content of 5% before it was filtered through a 0.45 µm syringe filter (Macherey-Nagel GmbH & Co. KG, Düren, Germany). The samples were analysed by an Inductively Coupled Plasma Atomic Emission Spectroscopy (ICP-OES) 5100 system including a SPR 4 auto-sampler from Agilent Technologies (Glostrup, Denmark), to determine the concentrations of calcium, magnesium, sodium, potassium and phosphorus. For detection, the wavelengths 396.85 nm, 279.55 nm, 588.99 nm, 769.90 nm and 213.62 nm were used. Standards obtained from Sigma-Aldrich (Saint-Quentin-Fallavier, France) were used to quantify the elements. All measurements were performed in triplicate.

### *2.13. Lactic acid and lactose composition on membranes surface*

To determine the concentration of lactic acid and lactose on the surface of the membranes, a piece of the membranes (23.1 $cm^2$) was submerged into MiliQ water in an Branson 2200 ultrasound chamber (Branson Ultrasonics Corporation, Connecticut, USA) for 4 h. The water containing the lactic acid and lactose was then filtered through a 45 µm syringe filter (Macherey-Nagel GmbH & Co. KG, Düren, Germany) before the organics were quantified by high-performance liquid chromatography (HPLC) using a HPLC RID (refractive index detector) from Agilent Technologies (Glostrup, Denmark) equipped with an Aminex HPX-87H Ion column from Bio Rad Laboratories (Hercules, CA, USA), as previously described Nielsen and co-authors [2]. As mobile phase, 5 mM $H_2SO_4$ was used at a flowrate of 0.6 mL/min. The analysis was run at room temperature. Standards of lactic acid and lactose from Sigma-Aldrich (Saint-Quentin-Fallavier, France) were used for quantification. All measurements were performed in triplicate.

### *2.14. Statistics*

The data in this study is presented as an average ± standard deviation. One-way analysis of variance (ANOVA) was used using Microsoft Excel software to determine significant differences which were declared at a probability level $P < 0.05$. Principal component analysis (PCA) was applied to evaluate effects of pretreating the acid whey with RO and applied current. Principal component analysis (PCA) is a statistical unsupervised machine learning algorithm used to reduce data based on

**Table 2**
Calcium, magnesium, potassium, sodium and total phosphorous found in the anion-exchange membranes (AEM) and cation-exchange membranes (CEM) after 95% demineralization of acid whey (AW) and RO pre-processed acid whey (ROAW) using underlimiting current density (UL), limiting current density (L) and overlimiting current density (OL).

| | | Ca | Mg | K | Na | P |
|---|---|---|---|---|---|---|
| | | (mM/100 g membrane) | | | | |
| AEM | Pristine | 0.1 ± 0.0$^{a}$ | 0.1 ± 0.0$^{a,b}$ | 0.8 ± 0.8$^{a}$ | 0.7 ± 0.4$^{a}$ | 0.2 ± 0.0$^{a,b}$ |
| | AW UL | 0.5 ± 0.2$^{b}$ | 0.3 ± 0.2$^{b,c}$ | 0.5 ± 0.5$^{a}$ | 1.4 ± 0.3$^{a}$ | 2.9 ± 1.1$^{a,c}$ |
| | AW L | 0.3 ± 0.0$^{b}$ | 0.2 ± 0.0$^{c}$ | 1.1 ± 0.4$^{a}$ | 1.0 ± 0.3$^{a}$ | 1.9 ± 0.2$^{b,c}$ |
| | AW OL | 0.3 ± 0.0$^{b}$ | 0.2 ± 0.0$^{a,c}$ | 1.3 ± 0.1$^{a}$ | 1.0 ± 0.4$^{a}$ | 2.0 ± 0.4$^{a,c}$ |
| | ROAW UL | 0.4 ± 0.3$^{b}$ | 0.6 ± 0.2$^{c,d}$ | 3.0 ± 2.0$^{a}$ | 1.0 ± 0.5$^{a}$ | 4.2 ± 1.7$^{a,c}$ |
| | ROAW L | 0.4 ± 0.0$^{b}$ | 0.0 ± 0.0$^{bd}$ | 1.5 ± 0.5$^{a}$ | 0.6 ± 0.1$^{a}$ | 3.3 ± 0.3$^{a,d}$ |
| | ROAW OL | 0.3 ± 0.1$^{b}$ | 0.0 ± 0.0$^{b,d}$ | 0.7 ± 0.6$^{a}$ | 0.5 ± 0.6$^{a}$ | 2.9 ± 1.6 $^{cd}$ |
| CEM | Pristine | 5.2 ± 0.4$^{a}$ | 0.8 ± 1.2$^{a}$ | 0.1 ± 1.3$^{a}$ | 213.3 ± 20.1$^{a}$ | 0.2 ± 0.2$^{a}$ |
| | AW UL | 53.4 ± 2.9$^{b,c,d}$ | 27.0 ± 1.8$^{b}$ | 16.0 ± 1.0$^{b}$ | 78.9 ± 0.6$^{b}$ | 0.9 ± 0.2$^{b,d}$ |
| | AW L | 55.9 ± 0.2$^{c}$ | 26.9 ± 0.2$^{b}$ | 13.5 ± 1.4$^{b}$ | 77.2 ± 0.6$^{b,c}$ | 0.7 ± 0.1$^{b}$ |
| | AW OL | 55.0 ± 4.3$^{b,c,d}$ | 27.3 ± 1.5$^{b}$ | 14.3 ± 1.8$^{b}$ | 79.5 ± 0.7$^{b}$ | 0.6 ± 0.0$^{b}$ |
| | ROAW UL | 57.6 ± 0.7$^{b,c}$ | 19.8 ± 15.1$^{b,c}$ | 14.3 ± 0.7$^{b}$ | 75.9 ± 0.1$^{c}$ | 1.5 ± 0.0$^{c}$ |
| | ROAW L | 59.9 ± 0.1$^{b,d}$ | 8.7 ± 0.0$^{c}$ | 13.4 ± 0.8$^{b}$ | 76.0 ± 1.5$^{b,c}$ | 1.3 ± 0.0$^{d}$ |
| | ROAW OL | 61.1 ± 0.4$^{d}$ | 8.6 ± 0.2$^{c}$ | 14.3 ± 0.2$^{b}$ | 75.9 ± 1.5$^{b,c}$ | 1.3 ± 0.1$^{c,d}$ |

$^{a\text{-}g}$, different letter in column indicates significant difference ($P < 0.05$).

variance across the datasets (while eliminating noise). It was applied to spectral data (FTIR and 2D fluorescence spectra independently) to compare and evaluate effects of pretreating the acid whey with RO and of applied current, as well as the efficacy of membrane cleaning procedures applied. The PCA analysis was performed in GNU Octave version 6.3.0 [24], using the PARAFAC algorithm from the n-way toolbox [25,26].

## 3. Results and discussion

### 3.1. Membrane characteristics

#### 3.1.1. Water contact angle

The contact angles of both sides of the IEMs were measured to assess the change in hydrophobicity of the membranes (Fig. 3), although it is important to take in account that the contact angle measurement does not only takes into account the hydrophobicity of a membrane but also its structural heterogeneity, which is especially important for heterogeneous membranes that have a certain degree of porosity, which can lead to an uneven distribution of fouling on the membrane surface. Taking this into account, the side facing the diluate of the AEM, the contact angle decreased most when treating ROAW. Here it was observed that the contact angle of the AEM was significantly different from the pristine AEM regardless of the current density used. This is in accordance with expectations, since the ROAW have a higher dry matter than the AW. For the non-concentrated AW, the contact angle did not change significantly except for the condition where OLCD has been used. Among the ROAW the largest decrease in contact angle, of the AEM side facing diluate, was also found when operating at OLCD. The lowest decrease was found when operating at LCD. Depending on the solution to demineralize and the degree of water splitting, the effect of electroconvection can be lower on the AEM compared to the CEM [27,28]. This might explain why the electroconvection generated during OLCD does not prevent a change in the contact angle of side of the AEM facing the diluate.

The contact angle on both sides of the CEM decreased regardless of the current density and the type of whey used. On the side facing the diluate the largest decrease was found when using OLCD for both AW and ROAW. Mainly minerals are expected to exist as fouling on the CEM. However, mineral solubility is very sensitive to the pH changes occurring during water splitting. A combination of the high concentration of minerals in AW [2] and the pH changes during OLCD may counterbalance the vortices occurring during electroconvection. For the CEM side facing the concentrate, no differences were found in the obtained water contact angle values between the current densities applied when treating AW. However, for the ROAW the lowest decrease in contact angle was found when using LCD. This may indicate that electroconvection does not prevent a decrease in hydrophobicity of the CEM. However, it is important to note that during cleaning and in the limiting and overlimiting current regimes, the IEM functional groups and surface can be altered/modified [33,44,45,46].

#### 3.1.2. Mineral concentration in the membranes

The mineral concentrations found in the membranes can be seen in Table 2. It is relevant to mention that the content of minerals in the membranes also reflects the transport of ions through the membranes. For example phosphorus is present in AEM because phosphate is a counter-ion for the AEM while calcium and magnesium are counter-ions for the CEM. Nevertheless, it allows to compare the different ED conditions and compare ED of ROAW with AW. As expected, the dominating mineral identified on the AEM is phosphorous, which is in agreement with expectations since phosphorous in milk exist as phosphate $PO_4^{3-}$ or protonated as $HPO_4^{2-}$ or $H_2PO_4^{-}$ depending on pH [29], and are thus migrating through the AEM, substituting the $Cl^-$ counter-ions initially compensating the positively charged quaternary ammonium fixed groups of the pristine membrane. No statistical significant difference ($p > 0.05$) among the phosphorous concentrations found for the AEM used for treating AW were observed. Nevertheless, the phosphorous concentration in the AEM where ULCD had been used was higher than that for the AEM, where LCD and OLCD were used. Furthermore, there was no statistic significant difference ($p > 0.05$) among the concentration of phosphorous on the AEM used for treating ROAW. The phosphorous concentration on the AEM was higher on the membranes used for treating ROAW compared to the AW, but a significant difference was only observed for LCD where 75% more phosphorous was found on the AEM used for treating ROAW. The higher concentration of phosphorous on the AEM used for ROAW can be explained by the higher concentration of phosphorous present in the ROAW compared to the AW.

The sodium, potassium and magnesium concentrations for the fouled AEM did not significantly differ from those of the pristine AEM. However, a slight increase in calcium concentration, independent of the current density and the whey type used, was observed for the fouled AEM, which could be explained by the pH increase occurring on the interface between the AEM and the liquid diffusion boundary layer of the concentrate solution [30]. The pH increase leads to complex formation and precipitation of calcium [31,32]. Contrarily, potassium and sodium are not affected to the same extent by pH changes and are thus primary present in their ionic forms [31], which may explain why they were not found in increased amounts in the AEM.

Sodium, calcium and magnesium were found in highest concentrations in the CEM. However, the sodium concentration in the fouled membranes was significantly lower than the sodium concentration in the pristine membrane. Dufton and co-authors [6] has previously reported similar results. The high sodium concentration in the pristine CEM may be explained by converting it into $Na^+$ form during the cleaning procedure with NaOH. Therefore the sodium concentration is higher for the pristine CEM than for the CEM after ED operation. Besides, it is difficult to infer if and how much of the sodium on the used CEM are

**Table 3**
Lactic acid and lactose found on the anion-exchange membranes (AEM) and cation-exchange membranes (CEM) after 95% demineralization of acid whey (AW) and RO pre-processed acid whey (ROAW) using underlimiting current density (UL), limiting current density (L) and overlimiting current density (OL).

| | | Lactic acid | Lactose |
|---|---|---|---|
| | | (mM/100 g membrane) | |
| AEM | Pristine | $0.0 \pm 0.0^{a}$ | $0.61 \pm 0.0^{a}$ |
| | AW UL | $5.6 \pm 0.0^{b,c}$ | $2.24 \pm 0.0^{b}$ |
| | AW L | $3.7 \pm 0.0^{d}$ | $2.21 \pm 0.0^{b,c}$ |
| | AW OL | $3.7 \pm 0.0^{d}$ | $1.87 \pm 0.01^{c}$ |
| | ROAW UL | $6.2 \pm 1.7^{e}$ | $3.74 \pm 0.01^{d}$ |
| | ROAW L | $7.5 \pm 0.0^{e}$ | $3.68 \pm 0.0^{d}$ |
| | ROAW OL | $5.0 \pm 0.0^{e}$ | $3.72 \pm 0.02^{d}$ |
| CEM | Pristine | $0.1 \pm 0.0^{a}$ | $0.59 \pm 0.02^{a}$ |
| | AW UL | $2.8 \pm 0.0^{b}$ | $2.54 \pm 0.0^{b}$ |
| | AW L | $2.4 \pm 0.0^{c}$ | $2.36 \pm 0.02^{b,c}$ |
| | AW OL | $2.2 \pm 0.0^{d}$ | $2.16 \pm 0.0^{c}$ |
| | ROAW UL | $5.2 \pm 0.0^{e}$ | $5.07 \pm 0.0^{d}$ |
| | ROAW L | $4.7 \pm 0.1^{e}$ | $4.66 \pm 0.03^{d}$ |
| | ROAW OL | $5.4 \pm 0.0^{e}$ | $4.35 \pm 0.0^{d}$ |

[a-l], different letter in column indicates significant difference ($P < 0.05$).

actual due to mineral fouling from the ED processing of AW and ROAW. A possible explanation may be the formation of a sodium analogue to the ammonium magnesium phosphate, struvite, that may precipitate in the membranes [40]. Another possible explanation is that the major part of sodium ions remain as counter-ions, as they are in high concentration in the product, they can compete with other cations (e.g., $K^{+}$ and $Ca^{2+}$) during their migration through the CEM and even at high demineralization degree, they are still available in the diluate and are transferred through the CEM. It has previously been reported that fouling on IEMs mainly consist of calcium and magnesium [9,10]. For AW the calcium concentration on the CEM was independent of the current density, while the calcium concentration increased with increasing current density for the ROAW. Interestingly, although the concentration of calcium in ROAW is about 2.5 times higher than the calcium concentration in AW, the difference in calcium concentration between ROAW and AW CEM membranes is at maximum 10%. Moreover, the magnesium concentration in the CEM was significantly lower (three times) for ROAW than AW when using LCD and OLCD. Water splitting at the depleted interface of a CEM produces $OH^{-}$ ions (due to their Donnan co-ion exclusion), which increases the pH at the diluate/membrane interface, thus causing formation of precipitates of carbonate and hydroxides of calcium and magnesium [33,47]. This effect is expected to be more pronounced in the ROAW due to its up-concentration compared to AW.

### 3.1.3. Lactic acid and lactose

The lactic acid and lactose concentration on the IEMs is shown in Table 3. Lactic acid was found on both the AEM and CEM. For both the AW and ROAW the lactic acid concentration was highest on the AEM. This is in compliance with expectations, since lactate is transported through the AEM. For AW the highest concentration of lactic acid on the AEM was observed when using ULCD, while there was no difference in the lactic acid concentration when using LCD and OLCD. For ROAW the lactic acid concentration was significantly less ($P < 0.05$) when using OLCD compared to LCD, probably because the generation of electroconvective vortices at OLCD disrupts the lactic acid fouling formation at IEMs surface [11,33].

The lactic acid concentration was also higher on the AEM used for ROAW compared to AW when using LCD and OLCD, because of the higher initial lactic acid concentration in ROAW than in AW. The presence of lactic acid on the CEM is likely a result of the high lactic acid concentration in the ED concentrate being in contact with the CEM, and is increasing with the RO pre-processing of the AW. Thus, residual compounds could be present in the membranes due to the contact with the solute ions and/or insufficient cleaning.

Lactose was observed on both the AEM and CEM after the ED processing. Lactose is a neutral compound, and is thus not transported through the IEMs by electromigration but by diffusion through both the AEM and CEM [34,35].

## 3.2. Visual inspection of membranes

A visual inspection of the membranes by imaging (Fig. 4) does not reveal any fouling of the CEM regardless of the current density used. However, an orange color change is observed on the AEM. It is well known, that riboflavin exists in large quantities in dairy products and it has a yellow to orange appearance [36]. Since riboflavin can exist as an anion, it may be transported towards the anode and attaches to the positively charged AEM. From the visual inspection of the AEMs it can be seen that for AW, the orange color is more pronounced when operating in OLCD, indicating more attachment of riboflavin. For ROAW the largest color change is observed when operating in ULCD, whereas the color change is hardly seen on the AEM used for OLCD. Electroconvection can explain the lower color change of the AEM used for treating ROAW using OLCD.

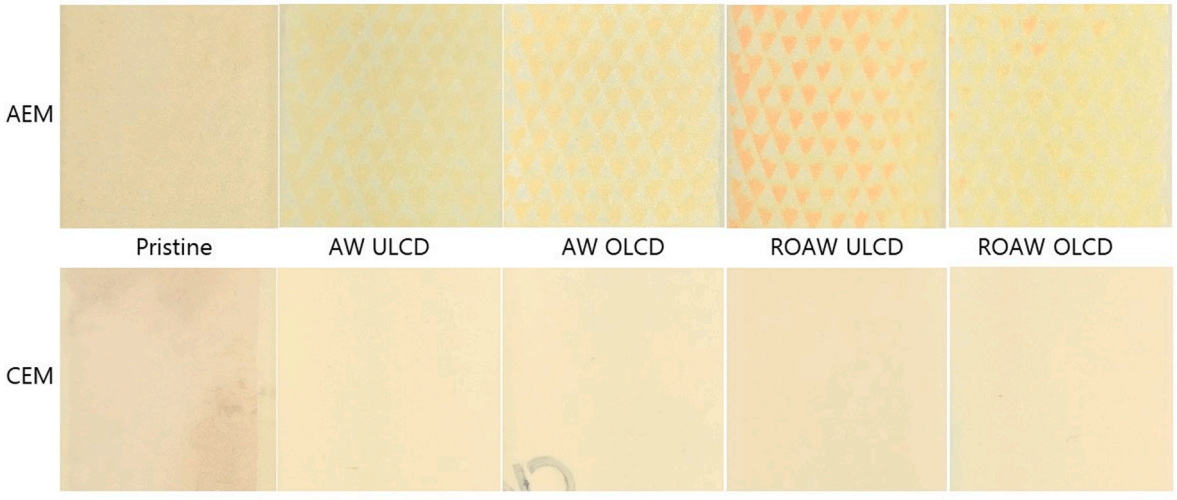


**Fig. 4.** Photos of pristine and acid whey (AW) and RO pre-processed acid whey (ROAW) fouled AEM and CEM side facing the diluate using underlimiting current density (ULCD) or overlimiting current density (OLCD).

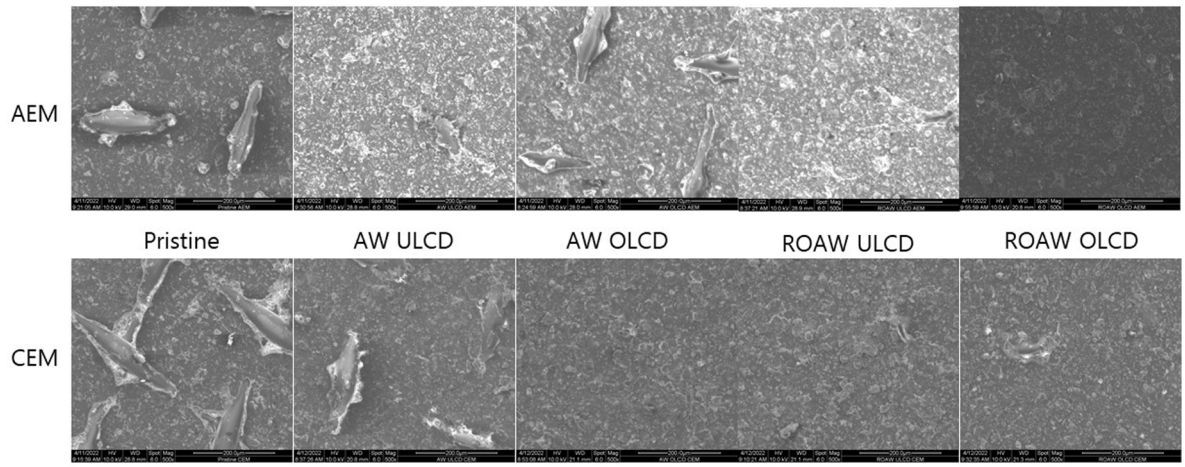


**Fig. 5.** SEM images of pristine and acid whey (AW) and RO pre-processed acid whey (ROAW) fouled AEM and CEM side facing the diluate using underlimiting current density (ULCD) or overlimiting current density (OLCD).

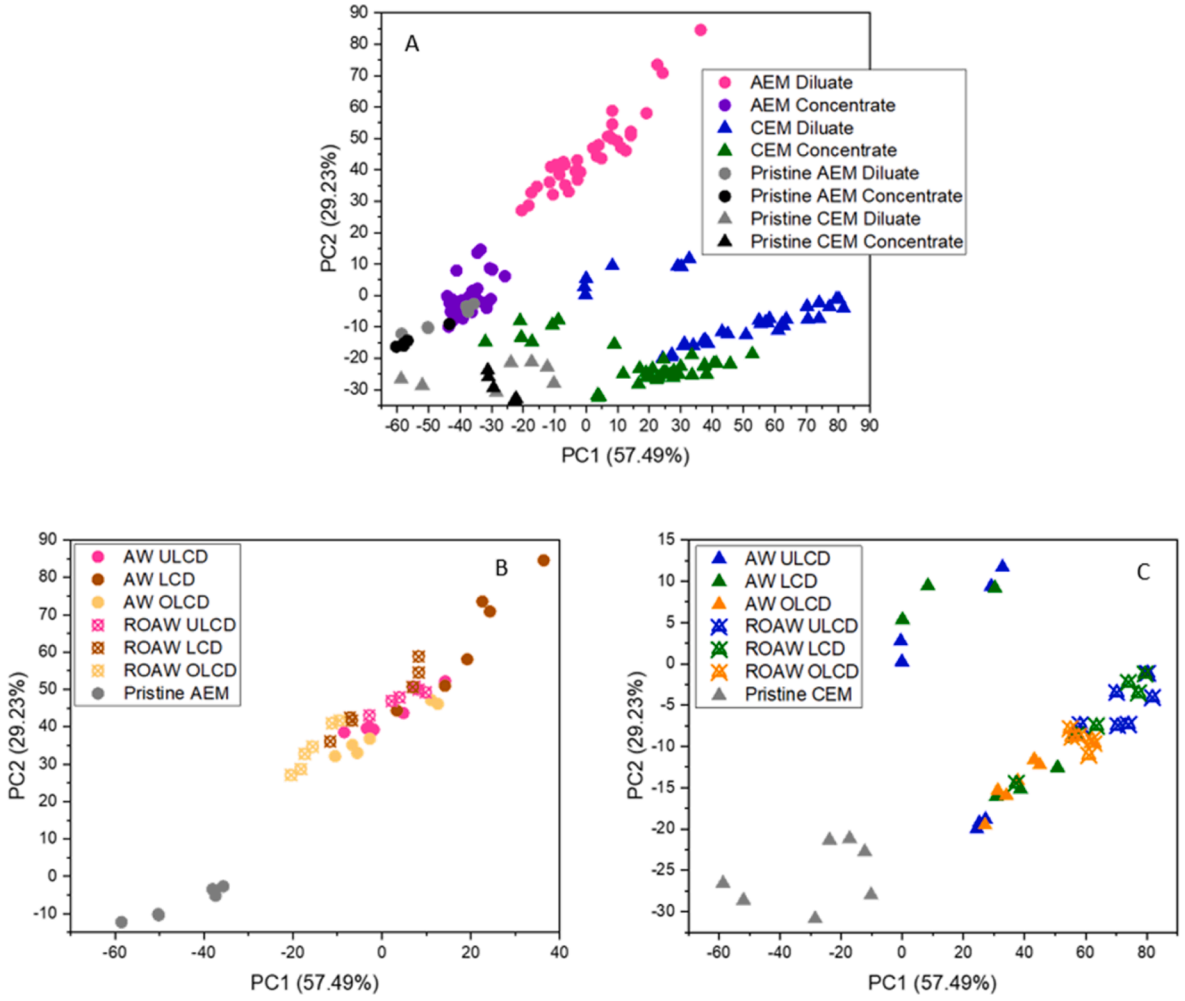


**Fig. 6.** Score plots between first two principal components (PCs) obtained by PCA of EEMs of A) all membrane surfaces acquired during the ED processing of AW and ROAW including pristine membranes, B) all AEM surfaces side facing the diluate obtained during the ED processing of AW and ROAW including information about applied current density and pristine membranes and C) all CEM surfaces side facing the diluate acquired during the ED processing of AW and ROAW including information about applied current density and pristine membranes.

### *3.3. Scanning electron microscopy*

SEM images of the IEMs side facing the diluate show that fouling is present on the AEM and CEM both when using ULCD and OLCD, after demineralization of AW and ROAW, since the backbone reinforcing net of the membranes are only visible on the pristine membranes (Fig. 5).

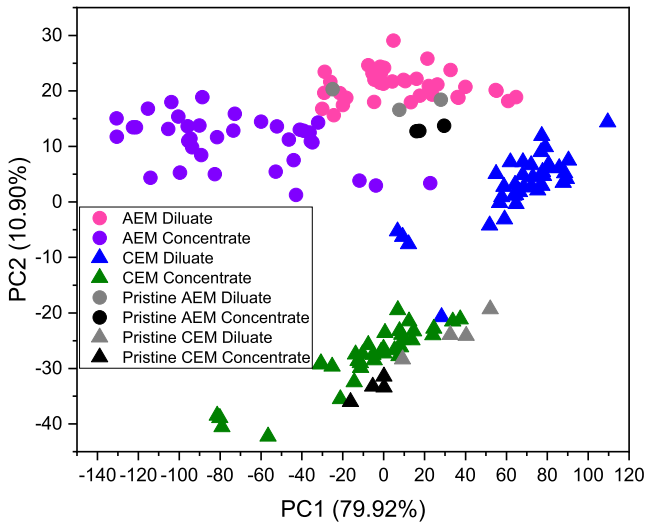


**Fig. 7.** Score plots between first two PCs obtained by PCA of FTIR signals of all membrane surfaces acquired during the ED processing of AW and ROAW including pristine membranes.

For the AW, less fouling is seen on the AEM when using OLCD compared to ULCD, while no significant differences can be observed on the CEM when using OLCD compared to ULCD. However, further studies should be done by analyzing the cross sections of the membranes.

### 3.4. 2D fluorescence spectroscopy

Fig. 6 shows the score plots of the first two principal components (PCs) values obtained by principal component analysis (PCA) for all fluorescence spectra of the membrane surfaces (example of a raw 2D fluorescence map can be seen in **S1**). Each point represents one EEM which was obtained from a given membrane surface. Fig. 6A shows the score plot of all membrane surfaces measured. From here it is evident that the AEMs group together as well as the CEMs also group together, meaning that there is a difference in the surfaces of the AEMs and CEMs. Within the AEM group, it can be seen that the sides of the AEM surfaces which have been in contact with the diluate are located more far away from the pristine AEM compared to the AEM surfaces which have been in contact with the concentrate solution. This indicates that the AEM surfaces which have been in contact with the diluate solution change more than the AEM surfaces which have been in contact with the concentrate solution during ED processing. The same applies for the CEM surfaces. Since minerals and organic matter are found on the AEM

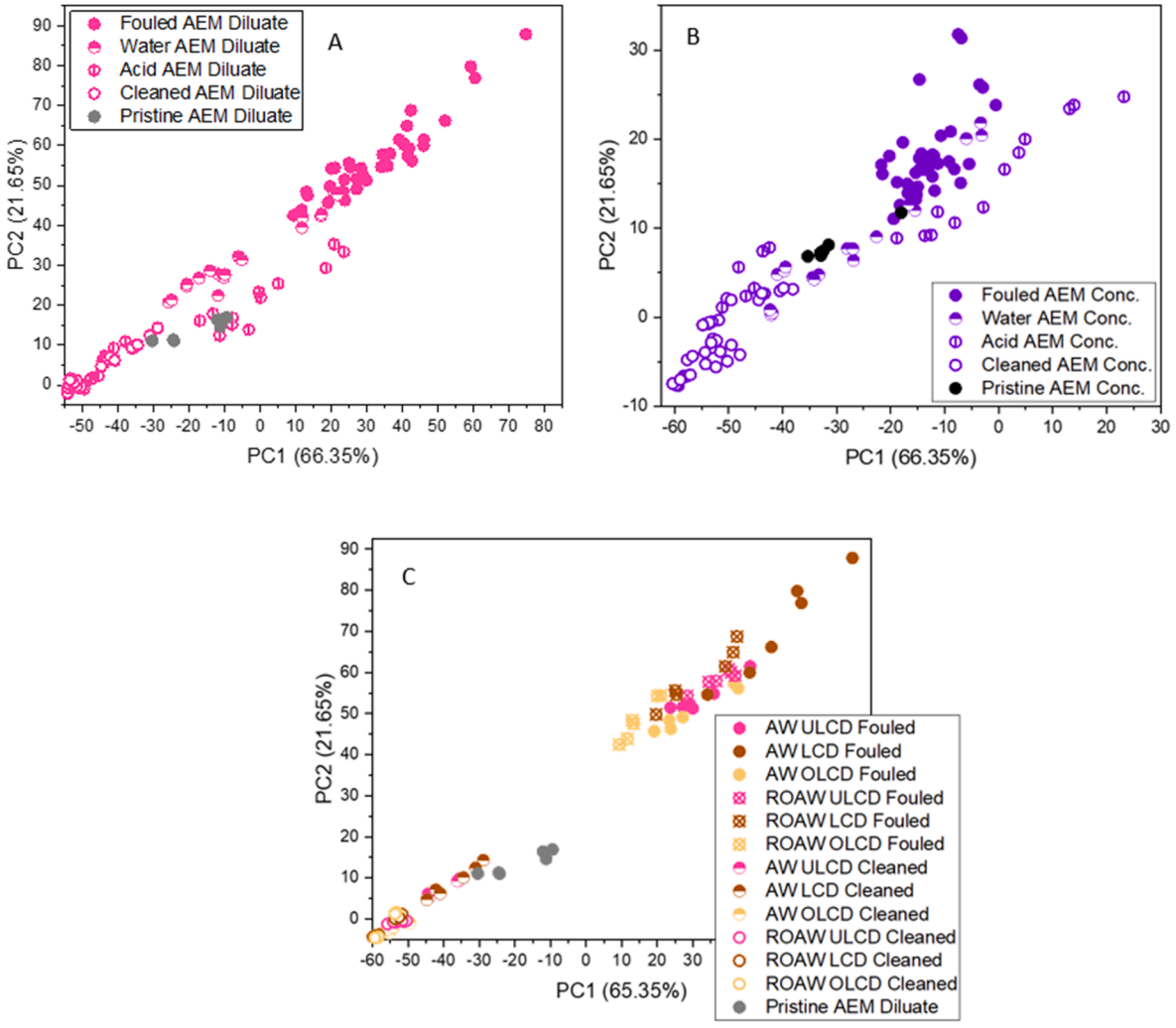


**Fig. 8.** Score plots between first two PCs obtained by PCA of EEMs of membranes before cleaning (fouled), after water flushing (water), after water flushing + acid cleaning + water flushing (acid) and after water flushing + acid cleaning + water flushing + alkaline cleaning (cleaned) for A) AEM which have been facing the diluate, B) AEM which have been facing the concentrate solution and C) AEM which have been facing the diluate solution including information about current density and type of diluate solution.

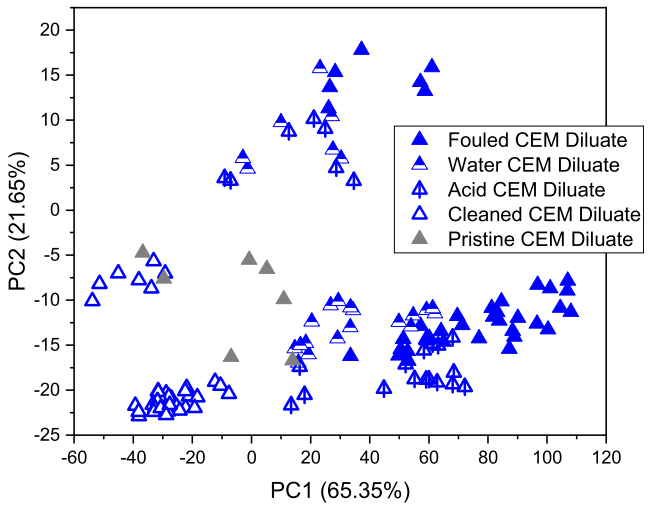


**Fig. 9.** Score plots between first two PCs obtained by PCA of EEMs of CEM which have been facing the diluate solution before cleaning (fouled), after water flushing (water), after water flushing + acid cleaning + water flushing (acid) and after water flushing + acid cleaning + water flushing + alkaline cleaning (cleaned) and including pristine CEM.

and CEM after ED processing, it is assumed that the observed changes in the membrane surfaces are correlated with fouling. The higher degree of fouling found on the membrane surfaces facing the diluate solution may be attributed to the electro-migrative and diffusive mass transport of cations and anions directed from the diluate to the concentrate side directed respectively to the cathode and the anode inducing concentration polarizations in the two liquid boundary layers near the respective CEMs and AEMs in contact with the diluate [9,11]. It is known that anion exchange membranes are more likely to be fouled by organic compounds because in water most of them are negatively charged [48,49]. On the other hand, for cation exchange membranes, concentration polarization can lead to mineral scaling. The latter effect is more pronounced for heterogenous (like those used in the present study) compared to homogenous membranes due to their higher electrical and geometric surface heterogeneity (which increases the non-uniformity in current density distribution) and weaker electro-convection [47].

Fig. 6B shows how the applied current density affects the fouling on the AEM surfaces side facing the diluate. It can be seen that OLCD of both AW and ROAW results in less fouling compared to LCD and ULCD. This is in compliance with the SEM images and with the concentrations of minerals found on the AEM as described in section 3.2.2. No clear effect is found for the RO pre-processing of the AW. For the side of the AEM facing the concentrate, no changes in the membrane surfaces were observed at varying current density and between AW and ROAW. The effect of RO pre-processing of AW and applied current density of the surface of the CEM can be seen in Fig. 6C. ROAW resulted in larger changes in the CEM surface than AW which are in accordance with the contact angle measurements and measured concentrations of calcium. An effect of the current density can also be observed for the ROAW. Here, as with the AEM, the OLCD resulted in least fouling of the CEM surface side facing the diluate, which also were reflected on the SEM images. The points which seem to be outliers on Fig. 6C is a result of color variation on the membranes which were already observed when the membranes were received from the supplier. Since fluorescence spectroscopy can detect color variation [37], these points are deviating from the remaining. No clear effect of RO pre-processing of AW and applied current density was found for the CEM surfaces side facing the concentrate. Common fluorophores in dairy products include peptides and riboflavin [38], which also are found in AW. The fluorescence spectra of the fouled membranes in contact with the diluate also showed the characteristic peak for amino acids at 280/325 nm of excitation/emission (data not shown). Furthermore, scaling causes color changes of the membranes. It is thus assumed that the compounds measured by fluorescence spectroscopy are peptides, riboflavin and minerals. This conclusion is supported by the analytical results of the minerals and by the visual inspection of the membranes.

### 3.5. *Fourier-transform infrared spectroscopy*

The score plot of the two first PCs values obtained by PCA of the signals acquired from FTIR of all measured membranes surfaces is shown in Fig. 7 (an example of the spectra can be found in **S2**). It can be seen that the AEM are grouping together and the CEM are grouping together as it also was found with the score plots of the two principal components (PCs) values obtained by PCA for all fluorescence spectra, meaning that differences between AEM and CEM are found with FTIR. In contrast to the results obtained from the fluorescence spectra, the FTIR cannot measure any differences between the AEM surfaces which have been in contact with the diluate and the pristine AEM. Instead, the AEM surfaces which have been in contact with the concentrate differed most from the pristine AEM. 2D fluorescence spectroscopy can capture not only information from natural fluorophores, but also from light interferences, such as color, presence of other compounds/structures that interfere with light path, or provoke light quenching. Therefore FTIR spectroscopy cannot be used to capture complex information regarding the interplay between different compounds; however, it can capture information regarding specific compounds that may not be reflected in fluorescence spectra.

FTIR spectroscopy can be used to detect lactic acid and carbohydrates [20,21], which are not fluorophores. Thus, it is suggested that the compounds measured by the FTIR spectroscopy are lactic acid and carbohydrates, such as lactose, which were found on the AEM and CEM. For the CEM most fouling was detected by the FTIR on the side facing the diluate, which could be due to lactose. The FTIR did not observe any differences in the AEM and CEM due to different current densities. This supports the conclusion that carbohydrates are among the compounds measured by the FTIR.

### 3.6. *Effect of cleaning procedure*

The score plots of the first two PCs values obtained by PCA for all fluorescence spectra of the pristine AEM and the fouled, water flushed, water flushed + acid cleaned + water flushed and water flushed + acid cleaned + water flushed + alkaline cleaned + water flushed AEM side facing the diluate are shown in Fig. 8A. It can be seen that the fouled membranes return back to the same condition as the pristine AEM after the first water flushing. This means that the fouling compounds detected by the fluorescence spectroscopy can be removed by water. Additional cleaning with acid only slightly affects the membranes, as a result of dissolution of remaining minerals by the acid. Further cleaning with an alkaline solution changes the membranes to a different state than the pristine membranes, and does not affect the removal of fouling. The same is observed for the AEM side facing the concentrate (Fig. 8B). Taking the RO pre-processing of the AW and the applied current density into account, it can be seen in Fig. 8C that the AEM which have been used to demineralize AW are more similar to the pristine AEM after the full cleaning procedure compared to the AEM which have been used for ROAW. There is no clear effect of the applied current density on the conditions of the AEM after the full cleaning procedure.

The score plots of the first two PCs values obtained by PCA for all fluorescence spectra of the pristine CEM and the fouled, water flushed, water flushed + acid cleaned + water flushed and water flushed + acid cleaned + water flushed + alkaline cleaned + water flushed CEM side facing the diluate (Fig. 9) are not giving as clear results as the score plots of the AEM (Fig. 8). It can still be concluded that water flushing removes most of the compounds measured by fluorescence spectroscopy, and the

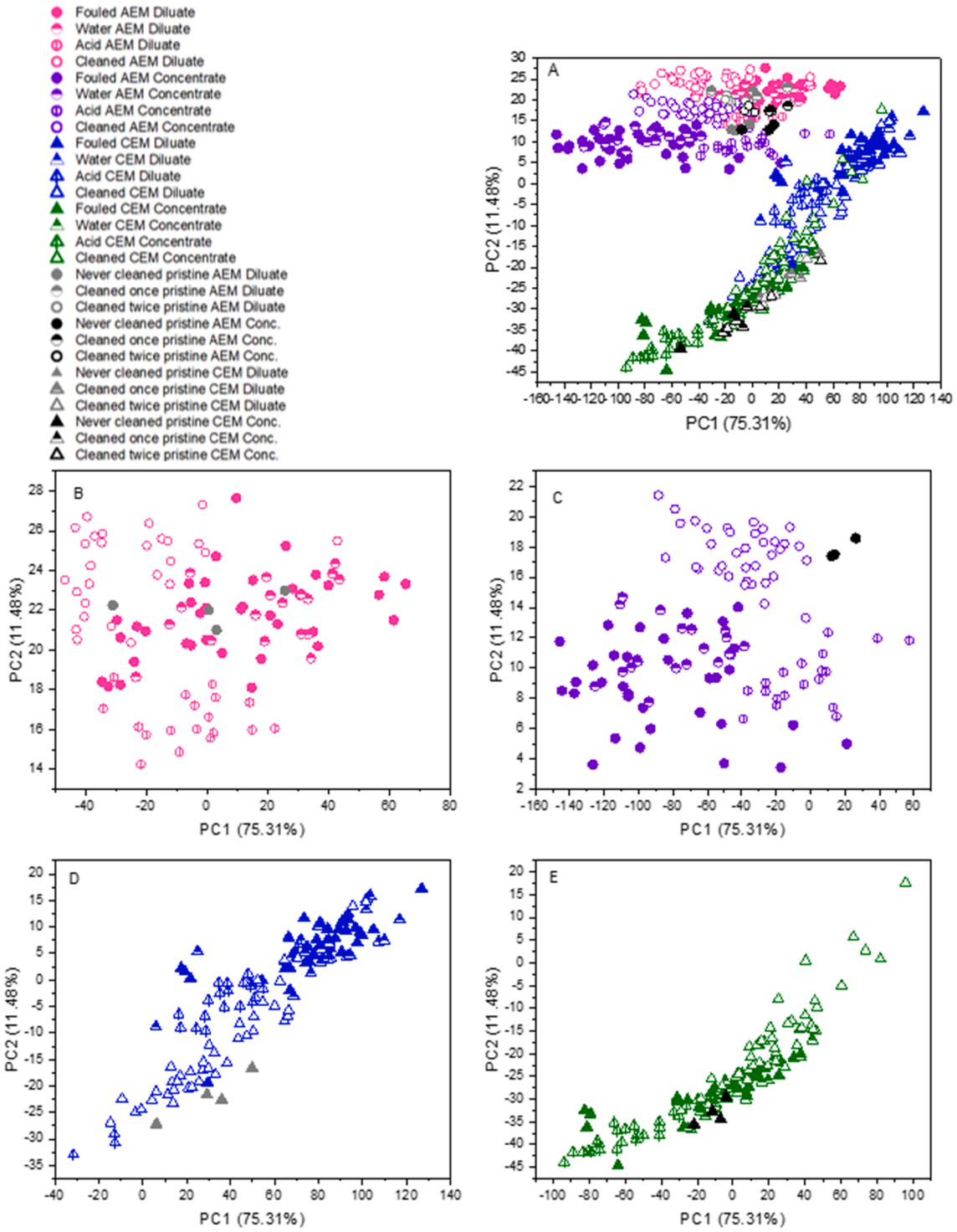


**Fig. 10.** Score plots between first two PCs obtained by PCA of FTIR signals of membranes before cleaning (fouled), after water flushing (water), after water flushing + acid cleaning + water flushing (acid) and after water flushing + acid cleaning + water flushing + alkaline cleaning (cleaned) for A) all membrane surfaces acquired during the ED processing of AW and ROAW, B) AEM which have been facing the diluate solution, C) AEM which have been facing the concentrate solution, D) CEM which have been facing the diluate solution and E) CEM which have been facing the concentrate solution.

cleaning with acid only slightly affects the membranes.

The rationale behind designing and performing these experiments was to explore the possibility to apply dedicated cleaning since the cleaning procedure for the concentrate and diluate compartments do not need to be necessarily the same, this facilitating the procedure and /or saving cleaning reagents. The results showed that for some of the membranes the full cleaning procedure is needed to restore the CEM to the pristine state. These CEM are those which had dark areas and came from a different batch of membranes. However, since fouling was not observed on the CEM side facing the concentrate, no effect of the different steps in the cleaning procedure was found for this side of the CEM. Nevertheless, the results obtained from the fluorescence spectroscopy show that water flushing is enough to remove most of the compounds fouling on the AEM and CEM, and acidic and alkaline

cleaning may not be necessary.

From the score plot of the two first PCs values obtained by PCA of the signals acquired from FTIR of all measured AEM and CEM before cleaning and after each step in the cleaning procedure (Fig. 10A), it can be seen that all measurements of the AEM are grouping together while the measurements of the CEM are grouping together. FTIR does not show any effect of the cleaning procedure on fouling removal on the AEM diluate side, as no differences between the pristine AEM and the fouled AEM side facing the diluate have been detected (Fig. 10B). However, it can be seen that cleaning with acid and alkaline changes the AEM side facing the diluate to a different state than the pristine AEM. Fig. 10C shows the effect of cleaning procedure on the AEM side facing the concentrate measured by FTIR. It can be seen that the full cleaning procedure is needed to remove the compounds detected by FTIR and restore the membranes to the original state. This finding supports the conclusion that the compounds detected by FTIR are lactic acid and lactose, since an alkaline cleaning step is needed to remove the compounds. The full cleaning procedure is also needed to clean the CEM side facing the diluate where lactose and other carbohydrates are expected to be found, while water flushing has no effect on removing the detected compounds (Fig. 10D). On the CEM side facing the concentrate no compounds have been detected by FTIR, showing no effect of the cleaning procedure on fouling removal on this side of the CEM. However, as with the AEM side facing the diluate, it can be seen that cleaning with acid and alkaline solutions changes the CEM side facing the concentrate to another state than the state of the pristine CEM (Fig. 10E).

The present results show that 2D fluorescence spectroscopy and FTIR can be used to detect the presence of different organic fouling and scaling (e.g., fluorophores, compounds associated to color change) on IEMs used for demineralizing AW and ROAW, and measure when the fouling has been removed during the cleaning procedure. Since fluorescence spectroscopy and FTIR detect different compounds of the fouling layer, the two methods are complementary and give the best results if combined. Although it does not provide specific and direct information about the species present, the PCA methodology is particularly useful to extract relevant information.

## 4. Conclusions

Although, pre-processing of acid whey by RO, compared to non-concentrated acid whey, can improve the energy efficiency in transporting ions during ED, the results of this study show that fouling of IEMs during ED processing of ROAW increases compared with AW that was not been concentrated, due to increased dry matter content in the diluate. In general, the concentrations of most fouling compounds was reduced when using OLCD compared to ULCD, due to the generation of electroconvective vortices. Fouling was observed for AEM and CEM and on both their surfaces facing the diluate and concentrate. A higher degree of fouling was found on the membrane surfaces facing the diluate solution, which can be attributed to the electro-migrative and diffusive mass transport of cations and anions directed from the diluate to the concentrate side directed respectively to the cathode and the anode inducing counter ion concentration polarizations in the two liquid boundary layers near the respective CEMs and AEMs in contact with the diluate. As expected, calcium and magnesium were primarily found in the CEM, while phosphorous, present in the form of negatively-charged phosphate species was found in the AEM, which is related to the transport of the respective counterions through these membranes. Lactic acid and lactose were found on both the AEM and CEM.

The analytical data obtained in the present study confirm the suitability and complementarity of 2D fluorescence spectroscopy and FTIR spectroscopy to monitor fouling in IEMs as well the feasibility of the applied cleaning procedures, thus opening the possibility to design dedicated IEM cleaning procedures for saving chemicals, since the cleaning procedure for the concentrate and diluate compartments do not need to be necessarily the same. Thus, the results obtained provide useful information to improve the efficiency of the ED acid whey treatment process, depending on the physicochemical properties of the diluate and process operating conditions employed.

## CRediT authorship contribution statement

**Emilie N. Nielsen:** Conceptualization, Data curation, Formal analysis, Investigation, Methodology, Validation, Writing – original draft, Writing – review & editing. **Ulysse Cordin:** Data curation, Formal analysis, Investigation, Writing – review & editing. **Mathias Gøtke:** Data curation, Formal analysis, Investigation, Writing – review & editing. **Svetlozar Velizarov:** Conceptualization, Investigation, Supervision, Writing – review & editing. **Claudia F. Galinha:** Conceptualization, Data curation, Investigation, Methodology, Supervision, Validation, Writing – review & editing. **Leif H. Skibsted:** Conceptualization, Data curation, Investigation, Methodology, Supervision, Validation, Writing – review & editing. **João G. Crespo:** Conceptualization, Investigation, Methodology, Supervision, Writing – review & editing. **Lilia M. Ahrné:** Conceptualization, Funding acquisition, Investigation, Methodology, Project administration, Resources, Supervision, Writing – review & editing.

## Declaration of Competing Interest

The authors declare that they have no known competing financial interests or personal relationships that could have appeared to influence the work reported in this paper.

## Data availability

Data will be made available on request.

## Acknowledgement

The authors would like to thank the staff at Hobro dairy for collection of acid whey samples. Also, special thanks to MemBrain s.r.o. and MEGA a.s. for providing us with the electrodialysis unit and the ion-exchange membranes. This present study is a part of the Platform for Novel Gentle Processing supported by the Dairy Rationalisation Fund (DDRF), Copenhagen University and Arla Foods. This work received support from PT national funds (FCT/MCTES, Fundação para a Ciência e Tecnologia and Ministério da Ciência, Tecnologia e Ensino Superior) through the projects UIDB/50006/2020 and UIDP/50006/2020.

## Appendix A. Supplementary material

Supplementary data to this article can be found online at https://doi.org/10.1016/j.seppur.2023.123814.

## References

[1] A.A. Alsaffar, Sustainable diets: The interaction between food industry, nutrition, health and the environment, Food Sci. Technol. Int. 22 (2) (2016) 102–111, https://doi.org/10.1177/1082013215572029.
[2] E.N. Nielsen, A. Merkel, S.R. Yazdi, L. Ahrné, The effect of acid whey composition on the removal of calcium and lactate during electrodialysis, Int. Dairy J. 117 (2021), https://doi.org/10.1016/j.idairyj.2021.104985.
[3] J. Chandrapala, R. Wijayasinghe, T. Vasiljevic, Lactose crystallization as affected by presence of lactic acid and calcium in model lactose systems, J. Food Eng. 178 (2016) 181–189, https://doi.org/10.1016/j.jfoodeng.2016.01.019.
[4] M. Saffari, T. Langrish, Effect of lactic acid in-process crystallization of lactose/protein powders during spray drying, J. Food Eng. 137 (2014) 88–94, https://doi.org/10.1016/j.jfoodeng.2014.04.002.
[5] G.Q. Chen, F.I.I. Eschbach, M. Weeks, S.L. Gras, S.E. Kentish, Removal of lactic acid from acid whey using electrodialysis, Sep. Purif. Technol. 158 (2016) 230–237, https://doi.org/10.1016/j.seppur.2015.12.016.
[6] G. Dufton, S. Mikhaylin, S. Gaaloul, L. Bazinet, How electrodialysis configuration influences acid whey deacidification and membrane scaling, J. Dairy Sci. 101 (9) (2018) 7833–7850, https://doi.org/10.3168/jds.2018-14639.

[7] G. Dufton, S. Mikhaylin, S. Gaaloul, L. Bazinet, Positive impact of pulsed electric field on lactic acid removal, demineralization and membrane scaling during acid whey electrodialysis, Int. J. Mol. Sci. 20 (4) (2019), https://doi.org/10.3390/ijms20040797.
[8] A. Merkel, D. Voropaeva, M. Ondrusek, The impact of integrated nanofiltration and electrodialytic processes on the chemical composition of sweet and acid whey streams, Journal of Food Engineering 298 (2021). https://doi.org/ARTN 110500. 10.1016/j.jfoodeng.2021.110500.
[9] S. Mikhaylin, L. Bazinet, Fouling on ion-exchange membranes: classification, characterization and strategies of prevention and control, Adv. Colloid Interface Sci. 229 (2016) 34–56, https://doi.org/10.1016/j.cis.2015.12.006.
[10] C. Casademont, M. Farias, G. Pourcelly, L. Bazinet, Impact of electrodialytic parameters on cation migration kinetics and fouling nature of ion-exchange membranes during treatment of solutions with different magnesium/calcium ratios, J. Membr. Sci. 325 (2) (2008) 570–579, https://doi.org/10.1016/j.memsci.2008.08.023.
[11] M. Persico, S. Mikhaylin, A. Doyen, L. Firdaous, V. Nikonenko, N. Pismenskaya, L. Bazinet, Prevention of peptide fouling on ion-exchange membranes during electrodialysis in overlimiting conditions, J. Membr. Sci. 543 (2017) 212–221, https://doi.org/10.1016/j.memsci.2017.08.039.
[12] M. La Cerva, L. Gurreri, M. Tedesco, A. Cipollina, M. Ciofalo, A. Tamburini, G. Micale, Determination of limiting current density and current efficiency in electrodialysis units, Desalination 445 (2018) 138–148, https://doi.org/10.1016/j.desal.2018.07.028.
[13] S. Pawlowski, C.F. Galinha, J.G. Crespo, S. Velizarov, 2D fluorescence spectroscopy for monitoring ion-exchange membrane based technologies - reverse electrodialysis (RED), Water Res. 88 (2016) 184–198, https://doi.org/10.1016/j.watres.2015.10.010.
[14] C.F. Galinha, G. Carvalho, C.A.M. Portugal, G. Guglielmi, M.A.M. Reis, J.G. Crespo, Two-dimensional fluorescence as a fingerprinting tool for monitoring wastewater treatment systems, J. Chem. Technol. Biotechnol. 86 (7) (2011) 985–992, https://doi.org/10.1002/jctb.2613.
[15] C.M. Andersen, G. Mortensen, Fluorescence spectroscopy: a rapid tool for analyzing dairy products, J. Agric. Food Chem. 56 (2008) 720–729.
[16] I. Merino-Garcia, F. Kotoka, C.A.M. Portugal, J.G. Crespo, S. Velizarov, Characterization of poly(Acrylic) acid-modified heterogenous anion exchange membranes with improved monovalent permselectivity for RED, Membranes (Basel) 10 (6) (2020), https://doi.org/10.3390/membranes10060134.
[17] G. Tiago, M.B. Cristovao, A.P. Marques, R. Huertas, I. Merino-Garcia, V.J. Pereira, J.G. Crespo, S. Velizarov, A Study on Biofouling and Cleaning of Anion Exchange Membranes for Reverse Electrodialysis, Membranes (Basel) 12(7) (2022). https://doi.org/10.3390/membranes12070697.
[18] Z. Movasaghi, S. Rehman, D.I. ur Rehman, Fourier Transform Infrared (FTIR) Spectroscopy of Biological Tissues, Applied Spectroscopy Reviews 43(2) (2008) 134-179. https://doi.org/10.1080/05704920701829043.
[19] R. Valand, S. Tanna, G. Lawson, L. Bengtstrom, A review of Fourier Transform Infrared (FTIR) spectroscopy used in food adulteration and authenticity investigations, Food Addit. Contam. Part A Chem. Anal. Control Expo. Risk Assess. 37 (1) (2020) 19–38, https://doi.org/10.1080/19440049.2019.1675909.
[20] Y. Lei, Q. Zhou, Y.-L. Zhang, J.-B. Chen, S.-Q. Sun, I. Noda, Analysis of crystallized lactose in milk powder by Fourier-transform infrared spectroscopy combined with two-dimensional correlation infrared spectroscopy, J. Mol. Struct. 974 (1–3) (2010) 88–93, https://doi.org/10.1016/j.molstruc.2009.12.030.
[21] A. Păucean, D.C. Vodnar, V. Mureşan, F. Fetea, F. Ranga, S.M. Man, S. Muste, C. Socaciu, Monitoring lactic acid concentrations by infrared spectroscopy: A new developed method for Lactobacillus fermenting media with potential food applications, Acta Aliment. 46 (4) (2017) 420–427, https://doi.org/10.1556/066.2017.0003.
[22] A. Merkel, A.M. Ashrafi, An investigation on the application of pulsed electrodialysis reversal in whey desalination, Int. J. Mol. Sci. 20 (8) (2019), https://doi.org/10.3390/ijms20081918.
[23] D.A. Cowan, J.H. Brown, Effect of turbulence on limiting current in electrodialysis cells, Ind. Eng. Chem. 51 (12) (1959) 1445–1448, https://doi.org/10.1021/ie50600a026.
[24] J.W. Eaton, GNU Octave (version 6.1.0), 2020. https://docs.octave.org/v6.1.0/. (Accessed 19th September 2022).
[25] R. Bro, PARAFAC. Tutorial and applications, Chemometrics and Intelligent Laboratory Systems 38(2) (1997) 149-171.
[26] C.A. Andersson, R. Bro, The N-way Toolbox for MATLAB, Chemom. Intel. Lab. Syst. 52 (1) (2000) 1–4.
[27] V.V. Nikonenko, N.D. Pismenskaya, E.I. Belova, P. Sistat, P. Huguet, G. Pourcelly, C. Larchet, Intensive current transfer in membrane systems: modelling, mechanisms and application in electrodialysis, Adv. Colloid Interface Sci. 160 (1–2) (2010) 101–123, https://doi.org/10.1016/j.cis.2010.08.001.
[28] J.H. Choi, H.J. Lee, S.H. Moon, Effects of electrolytes on the transport phenomena in a cation-exchange membrane, J. Colloid Interface Sci. 238 (1) (2001) 188–195, https://doi.org/10.1006/jcis.2001.7510.
[29] F. Gaucheron, The minerals of milk, Reprod. Nutr. Dev. 45 (4) (2005) 473–483, https://doi.org/10.1051/rnd:2005030.
[30] O.A. Rybalkina, M.V. Sharafan, V.V. Nikonenko, N.D. Pismenskaya, Two mechanisms of H+/OH− ion generation in anion-exchange membrane systems with polybasic acid salt solutions, J. Membr. Sci. (2022), https://doi.org/10.1016/j.memsci.2022.120449.
[31] F. Gaucheron, Milk Salts, distribution and analysis, 2011.
[32] J.S. Lindberg, M.M. Zobitz, J.R. Poindexter, C.Y. Pak, Magnesium bioavailability from magnesium citrate and magnesium oxide, J. Am. Coll. Nutr. 9 (1) (1990) 48–55, https://doi.org/10.1080/07315724.1990.10720349.
[33] S. Talebi, G.Q. Chen, B. Freeman, F. Suarez, A. Freckleton, K. Bathurst, S. E. Kentish, Fouling and in-situ cleaning of ion-exchange membranes during the electrodialysis of fresh acid and sweet whey, J. Food Eng. 246 (2019) 192–199, https://doi.org/10.1016/j.jfoodeng.2018.11.010.
[34] J. Chandrapala, G.Q. Chen, K. Kezia, E.G. Bowman, T. Vasiljevic, S.E. Kentish, Removal of lactate from acid whey using nanofiltration, J. Food Eng. 177 (2016) 59–64, https://doi.org/10.1016/j.jfoodeng.2015.12.019.
[35] J.-W. Lee, L.T.P. Trinh, H.-J. Lee, Removal of inhibitors from a hydrolysate of lignocellulosic biomass using electrodialysis, Sep. Purif. Technol. 122 (2014) 242–247, https://doi.org/10.1016/j.seppur.2013.11.008.
[36] D.R. Cardoso, S.H. Libardi, L.H. Skibsted, Riboflavin as a photosensitizer. Effects on human health and food quality, Food Funct 3 (5) (2012) 487–502, https://doi.org/10.1039/c2fo10246c.
[37] B.L. Ibey, H.T. Beier, V.S. Bagnato, V.H. Panhóca, M. Saito Nogueira, Fluorescence spectroscopy analysis of light-induced tooth whitening, Optical Interactions with Tissue and Cells XXX (2019).
[38] S. Shaikh, C. O'Donnell, Applications of fluorescence spectroscopy in dairy processing: a review, Curr. Opin. Food Sci. 17 (2017) 16–24, https://doi.org/10.1016/j.cofs.2017.08.004.
[40] C. K. Chauhan, M. J. Joshi Growth and characterization of struvite-Na crystals Journal of Crystal Growth, 401, (2014) 221-226. https://doi.org/10.1016/j.jcrysgro.2014.01.052.
[41] S. Pawlowski, C.F. Galinha, J.G. Crespo, S. Velizarov, 2D fluorescence spectroscopy for monitoring ion-exchange membrane based technologies – Reverse electrodialysis (RED), Water Res. 88 (2016) 184–198.
[42] A. Lejarazu-Larranaga, J.M. Ortiz, S. Molina, S. Pawlowski, C.F. Galinha, V. Otero, E. Garcia-Calvo, S. Velizarov, J.G. Crespo, Nitrate removal by donnan dialysis and anion-exchange membrane bioreactor using upcycled end-of life reverse osmosis membranes, Membranes 12 (2022) 101, https://doi.org/10.3390/membranes12020101.
[43] M. Cifuentes-Cabezas, C.F. Galinha, J.G. Crespo, M.C. Vincent-Vela, J.A. Mendoza-Roca, S. Alvarez-Blanco, Nanofiltration of wastewaters from olive oil production: Study of operatingconditions and analysis of fouling by 2D fluorescence and FTIR spectroscopy, Chem. Eng. J. 454 (2023), 140025.
[44] V.I. Zabolotskiy, A.Y. But, V.I. Vasil'eva, E.M. Akberova, S.S. Melnikov, Ion transport and electrochemical stability of strongly basic anion-exchange membranes under high current electrodialysis conditions, J. Membr. Sci. 526 (2017) 60–72, https://doi.org/10.1016/j.memsci.2016.12.028.
[45] L. Dammak, J. Fouilloux, M. Bdiri, C. Larchet, E. Renard, L. Baklouti, V. Sarapulova, A. Kozmai, N. Pismenskaya, A review on ion-exchange membrane fouling during the electrodialysis process in the food industry, Part 1: types, effects, characterization methods, fouling mechanisms and interactions, Membranes 11 (2021) 789, https://doi.org/10.3390/membranes11100789.
[46] Q. Xia, L. Qiu, S. Yu, H. Yang, L. Li, Y. Ye, Z. Gu, L. Ren, G. Liu, Effects of alkaline cleaning on the conversion and transformation of functional groups on ion-exchange membranes in polymer-flooding wastewater treatment: desalination performance, fouling behavior, and mechanism, Environ. Sci. Tech. 53 (24) (2019) 14430–14440, https://doi.org/10.1021/acs.est.9b05815.
[47] M.A. Andreeva, V.V. Gil, N.D. Pismenskaya, L. Dammak, N.A. Kononenko, C. Larchet, D. Grande, V.V. Nikonenko, Mitigation of membrane scaling in electrodialysis by electroconvection enhancement, pH adjustment and pulsed electric field application, J. Membr. Sci. 549 (2018) 129–140, https://doi.org/10.1016/j.memsci.2017.12.005.
[48] L. Zhang, H. Jia, J. Wang, H. Wen, J. Li, Characterization of fouling and concentration polarization in ion exchange membrane by in-situ electrochemical impedance spectroscopy, J. Membr. Sci. 594 (2020), 117443, https://doi.org/10.1016/j.memsci.2019.117443.
[49] H.-J. Lee, M.-K. Hong, S.-D. Han, S.-H. Cho, S.-H. Moon, Fouling of an anion exchange membrane in the electrodialysis desalination process in the presence of organic foulants, Desalination 238 (1–3) (2009) 60–69, https://doi.org/10.1016/j.desal.2008.01.036.

## Further reading

[39] X-C Liu and L. H. Skibsted Advances in understanding milk salts, In:Understanding and improving the functional and nutritional properties of milk, (2022), Huppertz, T. and Vasiljevic, T. (ed.), Burleigh Dodds Science Publishing, Cambridge, UK. https://doi.org/10.19103/AS.2022.0099.14.